Engineering Solid Mechanics 9 (2021) 299-310

Contents lists available at GrowingScience

Engineering Solid Mechanics

homepage: www.GrowingScience.com/esm

The impact of heat input on the mechanical properties and microstructure of High Strength Low Alloy steel welded joint by GMA welding process

Saadat Ali Rizvi[a*], Rajnish Singh[b] and Saurabh Kumar Gupta[c]

[a]*University Polytechnic, Jamia Millia Islamia,New Delhi-110025, India*
[b]*Department of Mechanical Engineering, Kamla Nehru Institute of Technology, Sultanpur,(UP), India*
[c]*Ministry of Indian Railway, India*

ARTICLEINFO

Article history:
Received 10 November 2020
Accepted 19 January 2021
Available online
19 January 2021

Keywords:
HSLA
Micro hardness
SEM
UTS
Microstructure
HAZ

ABSTRACT

The basic aim of this study was to find a relationship between heat input and mechanical properties of high strength low alloy steel (HSLA) welded joints and also elaborate its effect on microstructure. The combined effect of welding current, voltage and speed i.e. Heat Input on mechanical properties of High Strength Low Alloy Steel (ASTM A242 type-II) weldments have been studied in the present work. HSLA steel work pieces were welded by Gas metal arc welding (GMAW) process under varying welding current, arc voltage, and welding speed. Total nine samples were prepared at different heat input level i.e. 1.872 kJ/mm, 1.9333 kJ/mm, 2.0114 kJ/mm, 2.1 kJ/mm, 2.1956 kJ/mm, 2.296 kJ/mm, 2.4 kJ/mm, 2.5067 kJ/mm and 2.6154 kJ/mm It was observed that as heat input increases the ultimate tensile strength and microhardness of weldment decreased while impact strength increased and it was also observed that on increasing the heat input grain size of microstructure tends to coarsening it is only due to decreasing in cooling rate.

1. Introduction

Welding as one of the most important fabrication and maintenance processes has been playing an important role in the industrial and infrastructural development of any nation in the world. High strength low steel (HSLA) have been used in engineering machines parts, energy industries, and automobiles industries due to their high strength, low cost, and excellent weldability (Xue et al., 2003). Dong et al. (2014) investigated the effect of heat input on the mechanical quality and micro-structure of HSLA and they concluded that on increasing the welding heat input restrained the development of martensite and promoted the transformation of martensite to bainite and average hardness of HAZ decreased with increasing the welding heat input. Extensive research has been carried on the effect of heat input on micro-structure and mechanical properties of HSLA (Murti et al., 1993; Sampath, 2006). Heat input plays an important role in mechanical properties, residual stress and micro-structure of weldments (Taheri-Behrooz et al., 2018; Aliha & Gharehbaghi, 2017). From literature it was concluded that higher welding heat input led to more matrensite and higher the toughness (Li et al., 2018). Soria et al. (2019) concluded that the microstructure of lower zones was lath martensite while the upper and intermediate zones present a mixture of Widmastäten Ferrite, Acicular Ferrite and Martensite due to the most heat input supplied by the arc in the upper welding, obtaining less temperature gradient. Muthusamy et al. (2016) reported

* Corresponding author.
E-mail addresses: sarizvi1@jmi.ac.in (S. A. Rizvi)

doi: 10.5267/j.esm.2021.2.001

that on increasing in the heat input and temperature decreased the tensile strength of the weld joint. It was also noticed that rise in the heat input enhanced the toughness of weldment; it was only due to the increase in ferrite content in the matrix of martensite by enhancement of the heat input. It is also well known that increased heat input value promotes in cracking of weldment and heat affected zones (HAZ). Apart from this it is also well known that higher the value of heat input may introduce larger amounts of δ-ferrite contents in the weldments (Lippold, 2015; Woollin 2007). In some studies, hardness variation of welded joint was similar for all heat inputs and noticed its maximum value at coarse grained HAZ region (CGHAZ), while a soft zone appeared at the junction of HAZ and tempered zone of base metal while the tensile strength gradually decreased with the increase in heat input (Wen et al. 2018).

The aim of this research is to find a relationship between heat input and mechanical properties of HSLA welded joints and its effects on the microstructure. The combined effect of welding current, voltage and speed are studied.

2. Experiment detail

The parent metal (PM) used in this research was high strength low alloy (HSLA) steel plate of 200 mm × 60 mm × 10 mm size and welded by gas metal arc welding (GMAW). In the present work single V-groove is used so that welding could be accomplished in two numbers of passes ensuring full penetration. For welding Ador made a Ranger 403 model MIG welding machine. Welding current ranges from 100-350 A and voltage ranges from 16-39 volt for 1.2 mm filler wire. CO_2 gas is used as shielding gas. Gas supply is kept constant at 20 litre/min. Welding is performed in reverse polarity connection. The chemical composition of HSLA, filler wire used, and mechanical properties is listed in Tables 1 and 2, respectively.

Table 1. Chemical composition of parent metal and filler wire

Material	%C	% Cr	% Ni	% S	% Mn	% Cu	% Si	Fe
HSLA	0.17	0.04	0.05	0.05	1.35	0.028	0.48	Rest
Filler wire 308	0.035	18.5	8.5	0.04	1.55	0.02	---	

Table 2. Mechanical properties of base metal

Material	Yeild strength (MPa)	Ultimate strength (MPa)	% Elongation	Toughness (J)	Hardness (HV)
HSLA	315	478	50	105	90

V-groove and experimental setup used in this study is shown in Figs.1 and 2, respectively. Tensile test specimens were fabricated as per ASTM A242 type-II and nine tensile test samples at different heat input are shown in Fig. 3.

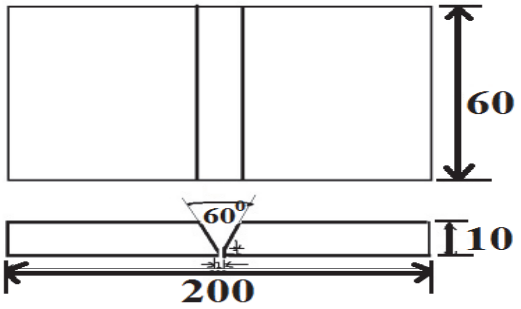

Fig. 1. Groove detail of sample (all dimension in mm).

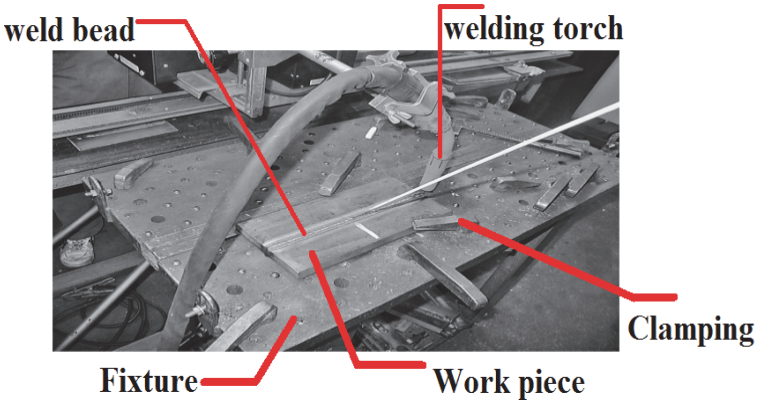

Fig. 2. Welding Setup.

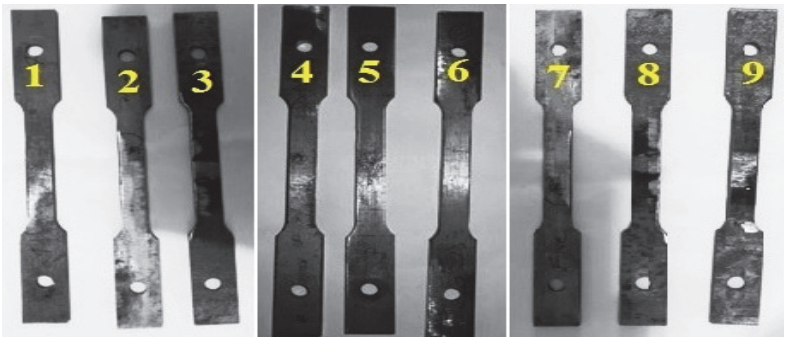

Fig. 3. Tensile sample specimen.

Table 3 presents the different parameters applied to the heat source and nine different heat inputs were used. The current was varied from 130 amperes to 250 amperes with increment of 15 ampere in each heat input level. Arc voltage is varied from 18 Volt to 34 Volt with increment of 2 Volt in each heat input level.

Table 3. Parameters and welding conditions

Sample No	Welding current (A)	Arc voltage (V)	Heat input (Kj/mm)
1	130	18	1.872
2	145	20	1.9333
3	160	22	2.0114
4	175	24	2.1
5	190	26	2.1956
6	205	28	2.296
7	220	30	2.4
8	235	32	2.5067
9	250	34	2.6154

The welded joints prepared under the different heat input level having different values of hardness, impact strength and tensile strength. Microstructures of weld zone also show varying trend for different current, voltage and welding speed combination i.e. heat input.

Table 3. Parameters used for MIG welding process to obtain various heat input condition

Welding current (A)	Arc Voltage (V)	Shielding gas flow rate (l/min)	Wire feed speed (IPM)
200	20	10	250

3. Result and discussion

3.1. Effect Heat Input on Absorbed Energy of Weld Zone

Fig.4 shows the effect of heat input on impact strength (Zhu et al., 2015). It is evident from the figure that with the increase in heat input, absorbed energy of weldments also increases. This may be due to increased grain size of ferrite with increase in current and voltage. This behaviour is due to coarsening of grain with increasing current and voltage. As current and voltages increase, heat input also increases. There is a decrease in rate of cooling of the weld pool, which yields a coarse structure which is soft. Larger grains have more ductility than smaller grains so toughness is higher for larger grains and increases with increasing grain size. From the toughness test data it has been observed that as heat input increases it affects the toughness of weldments. A graph has been plotted between Absorbed Energy vs Heat Input which is shown in Fig. 4.

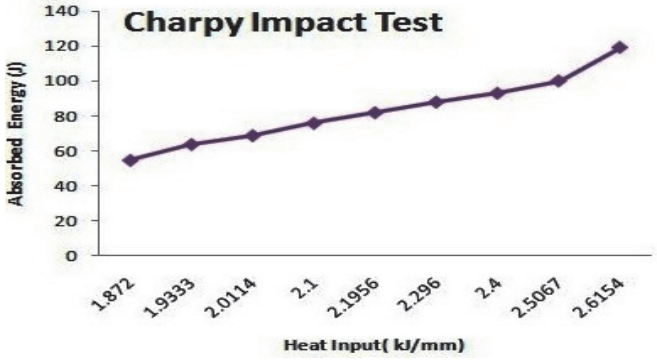

Fig. 4. Variation of Absorbed Energy with Heat Input.

The Charpy toughness test samples of weldments were tested at room temperature and it is observed that all samples were fractured from the centre shown in Fig. 5 with brittle fracture with little ductility (Shrikrishna et al., 2015).

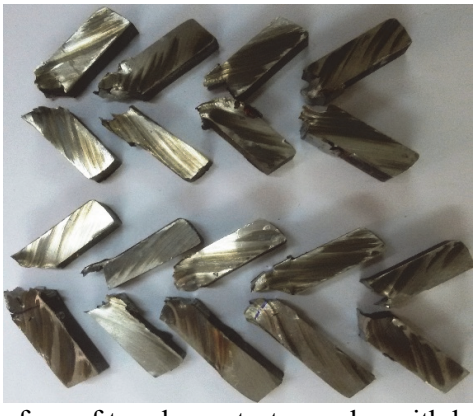

Fig. 5. Fracture surface of toughness test samples with location of fracture.

3.1.2 Effect Heat Input on Tensile Strength

The transverse tensile strength of all the joints made using different heat input conditions has been evaluated. In each condition two specimens were tested and the average tensile strength of two specimens shown in Fig. 3 per heat input is mentioned in Table 4 and it is also observed that on increasing the heat input value mechanical properties and microstructure of weldment (WM) and heat affected zone (HAZ) affected (Prasad & Dwivedi, 2008).

Table 4. Weld Joint Efficiency with welding Parameters

Specimen No.	Total Heat Input(kJ/mm)	Ultimate Tensile Test (MPa)	Joint Efficiency (%)
1	1.872	518	108.36
2	1.9333	513	107.32
3	2.0114	507.8	106.23
4	2.1	504.6	105.56
5	2.1956	501.1	104.83
6	2.296	497.7	104.12
7	2.4	494	103.34
8	2.5067	492.1	102.94
9	2.6154	489.3	102.36

Fig. 6 shows the combined effect of voltage, current and welding speed i.e. heat input on ultimate tensile strength of weld zone. The curve shows a decreasing trend for tensile strength (Prasad & Dwivedi, 2008). This indicates that high tensile strength and ductility is possessed by the joints at low heat input, which can be attributed to smaller dendrite sizes and lesser inter-dendritic spacing in the fusion zone. Relatively lower tensile strength and ductility is possessed by the joints with long dendrite sizes and large inter-dendritic spacing in the fusion zone of the joint welded using high heat input. Further it is found that all the tensile specimens fractured in the base metal which indicates that weld metal in all the joints possessed higher tensile strength than the base metal joint efficiency (%) shown in Table 4.

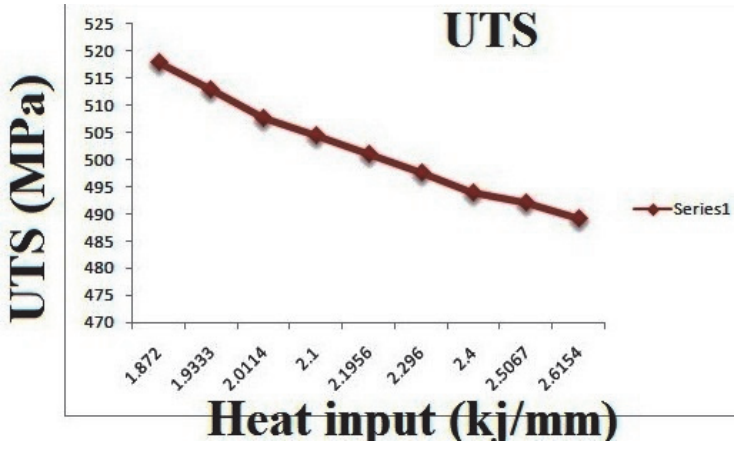

Fig. 6. Variation of Ultimate Tensile Strength with Heat Input

3.2. SEM Fractograph of Fractured Surface of Tensile Test Sample

The fractured surfaces of the tensile specimens were analysed using Scanning Electron Microscope (SEM). Figs. 7 to 15 show the SEM Fractograph images of all fractured surfaces of tensile test specimens. The fracture surface appeared as mixed mode, irrespective of heat input and temperature. Dimples of varying size and shape were observed in all the fractured surfaces which indicate that major fracturing mechanism was ductile and if dimple size is finer, the strength and ductility of the welded joints are higher (Nathan et al., 2015). From Fig. 7 it is observed that the fractured surface of the specimen at low heat input contains a large population of small and shallow dimples which is indicative of its relatively high tensile strength and ductility. From Fig. 8 to Fig. 15 it is observed that as heat input increases coarse and elongated dimples are observed. It is also observed that small dimples are surrounded by the large ones in all the specimens and a small quantity of tearing ridge is also present.

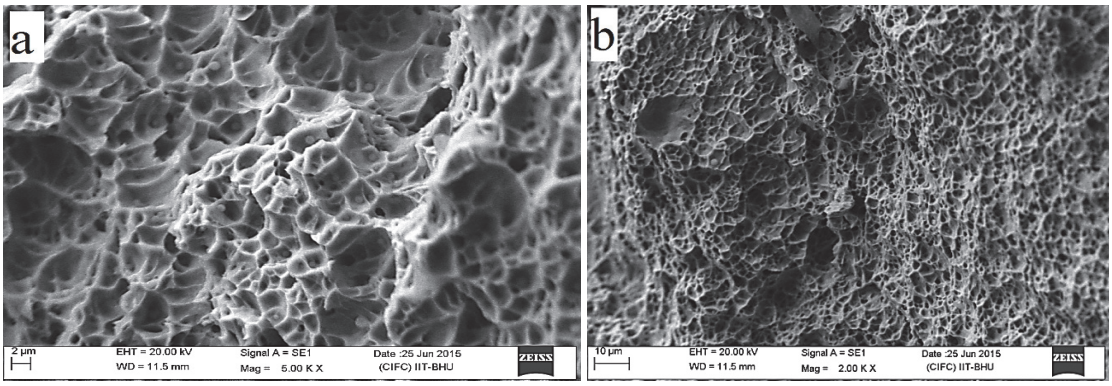

Fig. 7. SEM Fractograph of the Tensile Specimen No. 1 (a) at 5000X (b) 2000X

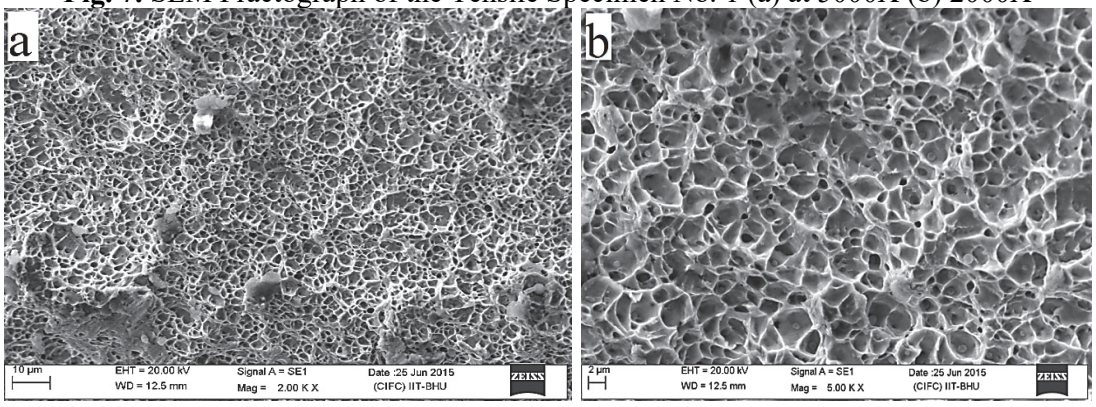

Fig. 8. SEM Fractograph of the Tensile Specimen No.2 (a) at 2000X (b) 5000X

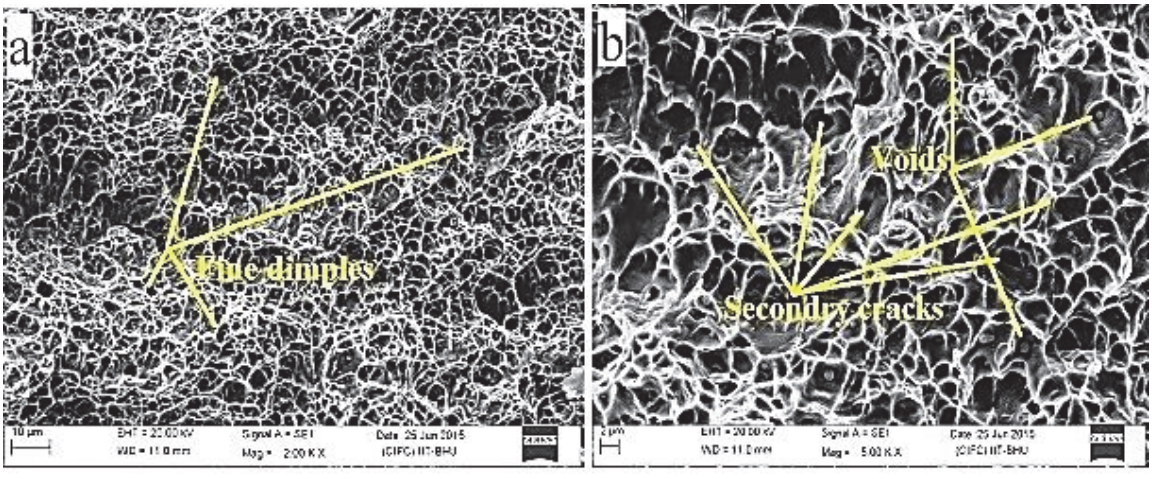

Fig. 9. SEM Fractograph of the Tensile Specimen No.3 (a) at 2000X (b) 5000X

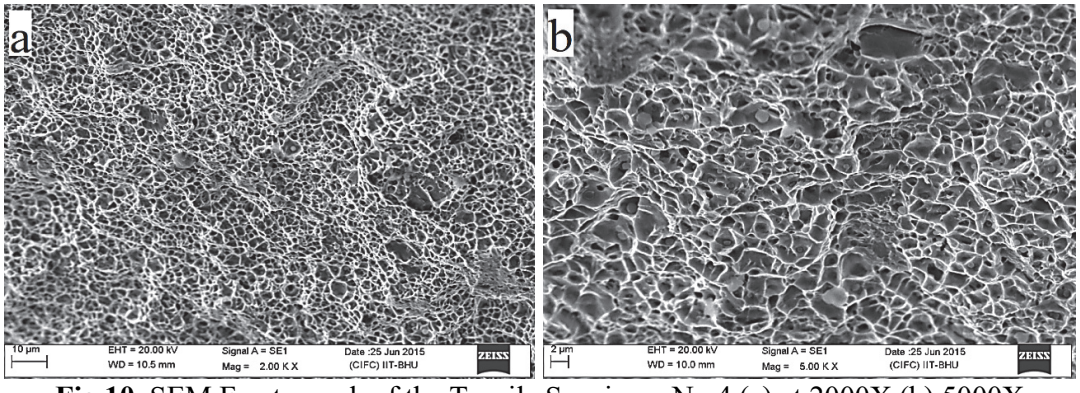

Fig.10. SEM Fractograph of the Tensile Specimen No.4 (a) at 2000X (b) 5000X

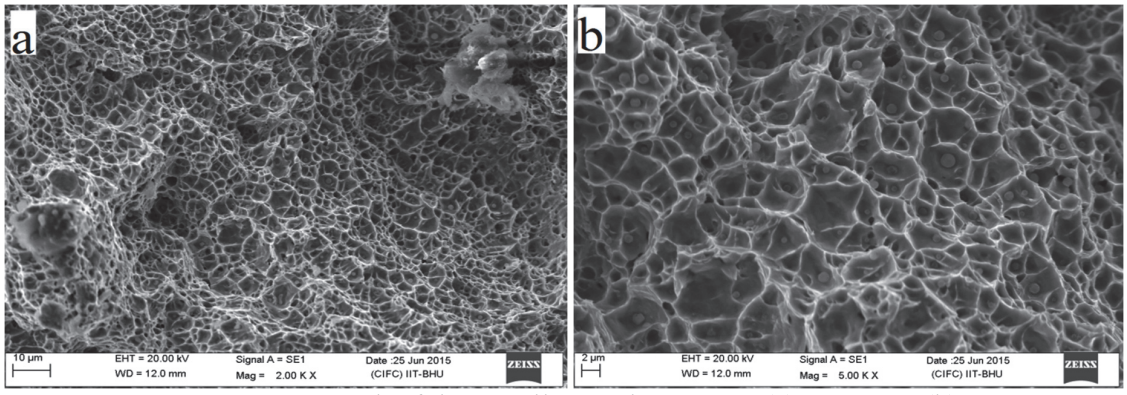

Fig.11. SEM Fractograph of the Tensile Specimen No.5 (a) at 2000X (b) 5000X

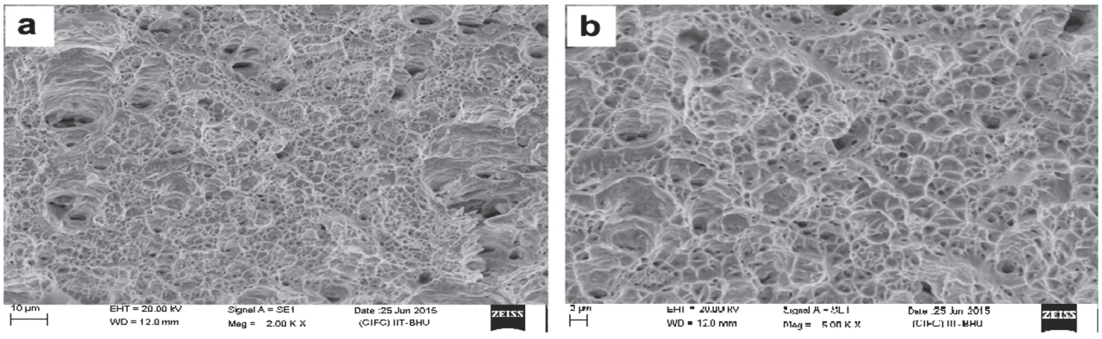

Fig. 12. SEM fractograph of the Tensile Specimen No.6 (a) at 2000X (b) 5000X

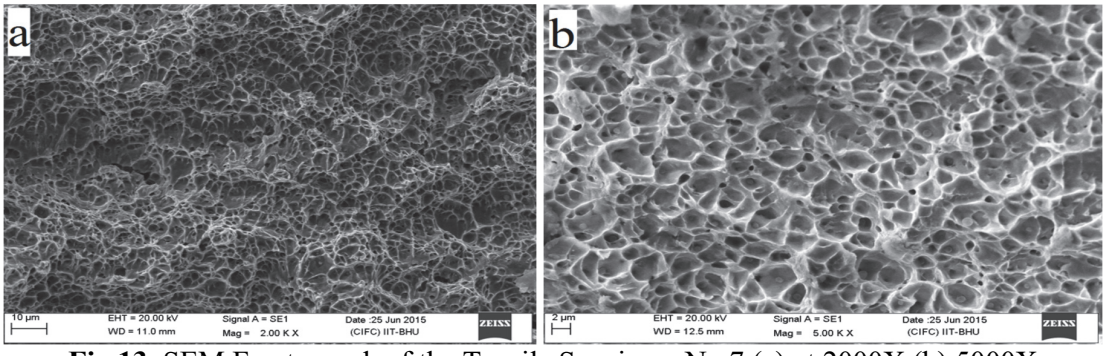

Fig.13. SEM Fractograph of the Tensile Specimen No.7 (a) at 2000X (b) 5000X

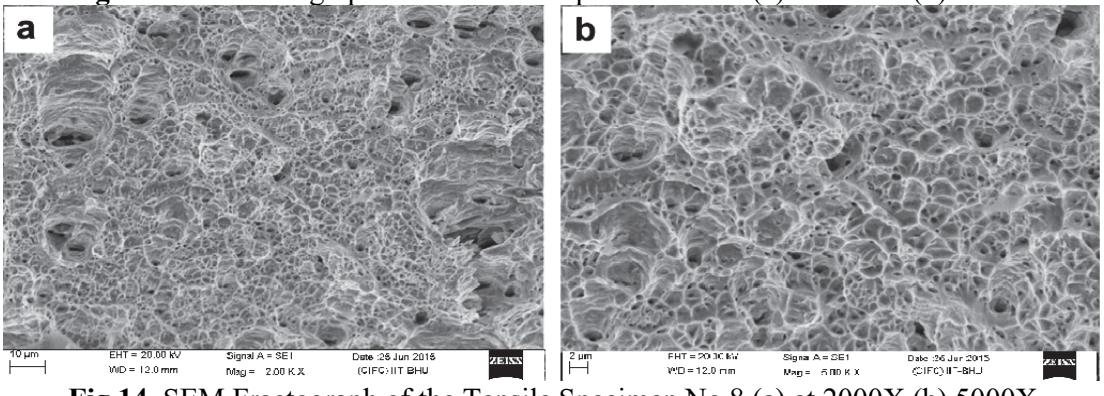

Fig.14. SEM Fractograph of the Tensile Specimen No.8 (a) at 2000X (b) 5000X

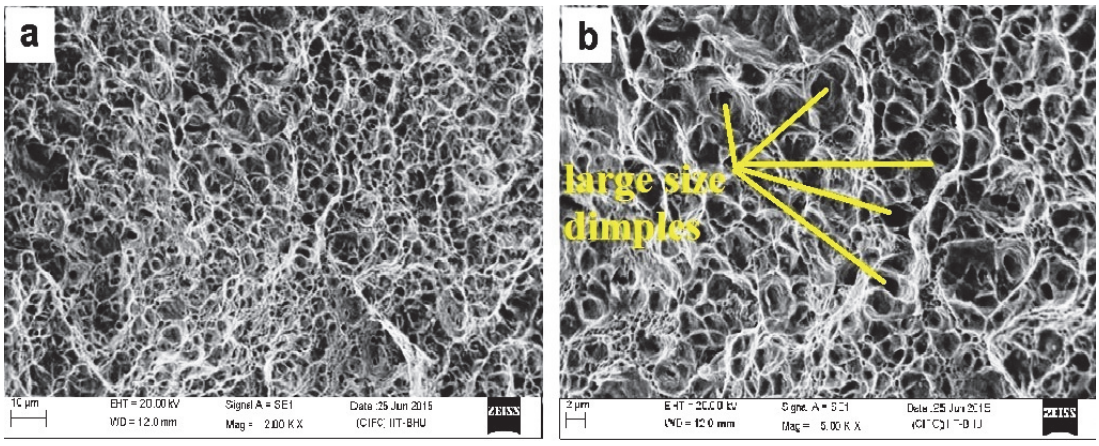

Fig.15. SEM Fractograph of the Tensile Specimen No.9 (a) at 2000X (b) 5000X

3.4 Micro-hardness of weld zone

The micro-hardness of the different weldment zone is measured by using Vicker's micro-hardness testing machine at load of 0.5 kg and dwell period of 10 second. Measurement of micro-hardness has been taken in two directions firstly in the transverse direction i.e. perpendicular to the base plate surface and secondary, in the longitudinal direction (lateral direction) i.e. parallel to the base plate surface and same are shown in Fig. 16 and Fig. 17 of respective test sample.

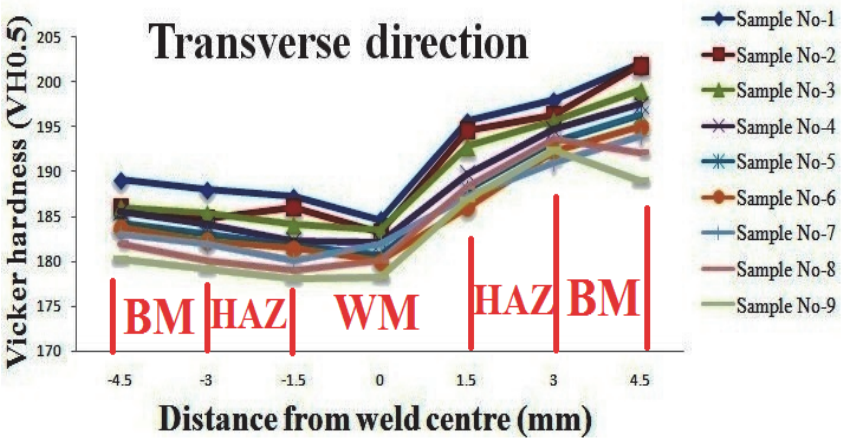

Fig. 16. Micro-hardness distribution of weld in transverse direction

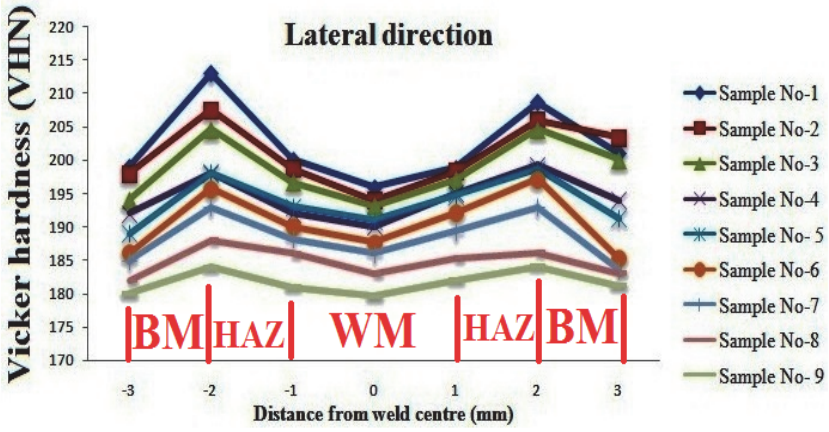

Fig. 17. Micro-hardness distribution of weld in lateral direction

Fig.16 shows that the micro hardness near the top of the weld bead surface is high and as the centre of the fusion/weld zone is approached by the indenter it gradually reduces, which is due to the fact that cooling rate is relatively higher at the top of the weld bead surface than at the centre of the weld metal (Njock Bayock et al., 2019). Any increase in the heat input has an inverse effect on the hardness of welded metal and it's HAZ. As an example, elevation of heat input from 1.872 kJ/mm to 2.6154 kJ/ reduced the hardness from 202 HV to 189 HV HB near top of the weld bead. Fig.16 it is observed that as the indenter traverses outwards (parallel to the base plate surface) from the centre of the weld/fusion zone towards the fusion boundary, micro hardness increases from 196 HV to 208.7 HV for sample no.1 (1.872 kJ/mm). As heat input increases from 1.872 kJ/mm to 2.6154 kJ/mm, the micro-hardness at weld centre decreases from 196 HV to 179.6 HV and at near fusion boundary it decreases from 208.7 HV to 184.1 HV. High hardness as possessed by the fusion boundary zone (FBZ) in all the joints can be attributed to the presence of acicular ferrite and partially un-melted grains at the fusion boundary which are partially adopted as nuclei by the new precipitating phase of the weld metal during the solidification stage. After reaching this peak value micro hardness shows a decreasing trend in the HAZ. In all the joints, HAZ area adjacent to the fusion boundary was coarse grained HAZ (CGHAZ) which possessed low hardness whereas the HAZ area adjacent to the base metal was fine grained HAZ (FGHAZ) which possessed high hardness (Grajcar et al. 2014). The reason for this trend of micro hardness in the HAZ of all the joints is that the area adjacent to the weld/fusion zone experiences relatively slow cooling rate (Miletić et al. 2020). Hence has coarse grained microstructure, whereas the area adjoining the base metal undergoes high cooling rate due to steeper thermal gradients and consequently has fine grained microstructure. This is evident from the trend depicted by the micro hardness profile within the HAZ of each of these joints. It is also observed that there is significant grain coarsening in the HAZs of all the joints. Further it is observed from the optical micrographs shown from Fig.16 and Fig.17 that the extent of grain coarsening in the HAZ increases with increase in heat input.

3.5 Microstructural Examination

In the present case metallographic photographs have been taken at two different places of six samples. First one was in a weld metal centre and the second one was in fusion boundary. Metallographic images of sample no.1, 2, 4, 5, 6, 7, 8, and sample no 9 have been taken and shown in Fig. 18 to Fig. 23. The weld metal centre has got somewhat complex structures consisting of columnar grains, elongated dendrites, and ferrite having no grain boundaries. The microstructure consists of acicular ferrite, Widmanstaten Ferrite and polygonal ferrite (Murti et al., 1993, Wen et al., 2018). In some cases bainite structure is also found. As heat input is increased the grain size of ferrite increases leading to decrease in hardness (Fig. 18 to Fig. 23). It is observed from these optical micrographs that as heat input increases the dendrite size and inter-dendritic spacing in the weld metal also increase. This dendrite size variation can be attributed to the fact that at low heat input, cooling rate is relatively higher due to which steep thermal gradients are established in the weld metal, which in turn allow lesser time for the dendrites to grow (Dong et al. 2013). This may be due to the fact that increases in heat input energy which in turn reduces cooling rate which results in decrease in hardness and increase in impact strength of weldment.

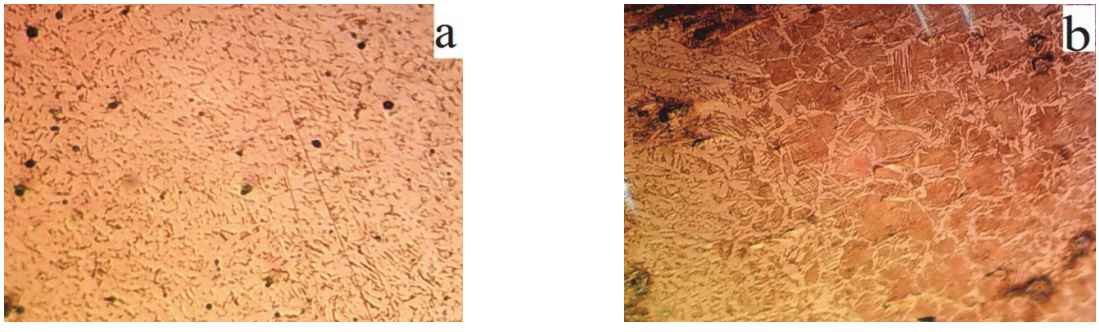

Fig.18. Microstructure of Sample No.1 (a) weld zone (100X) (b) fusion boundary (100X)

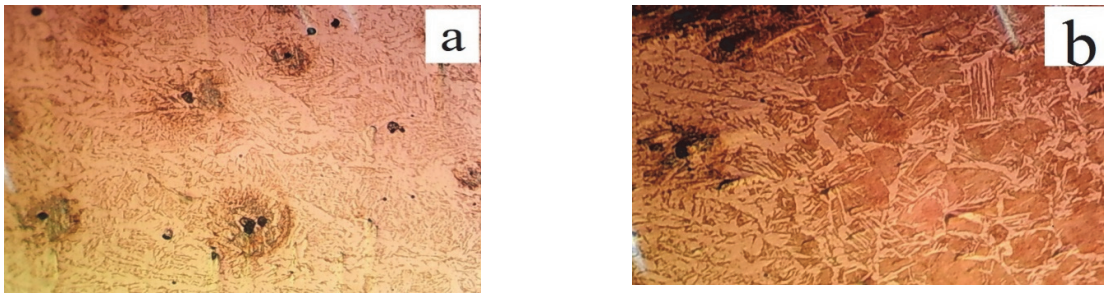

Fig.19. Microstructure of Sample No.2 (a) weld zone (100X) (b) fusion boundary (100X)

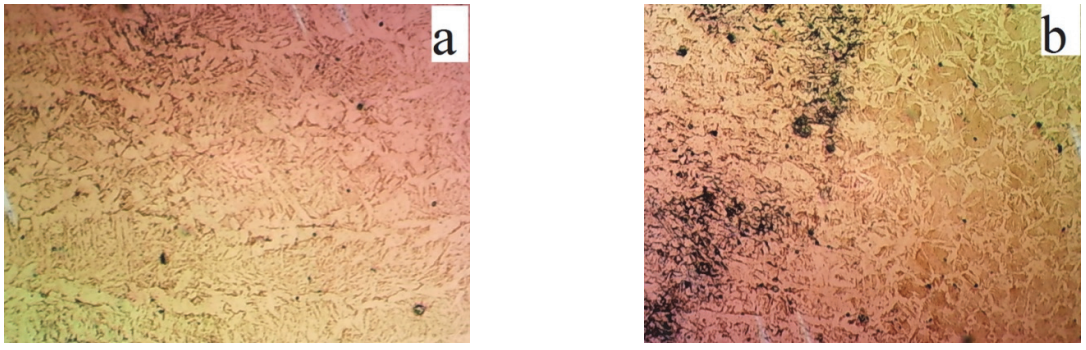

Fig. 20. Microstructure of Sample No.4 (a) weld zone (100X) (b) fusion boundary (100X)

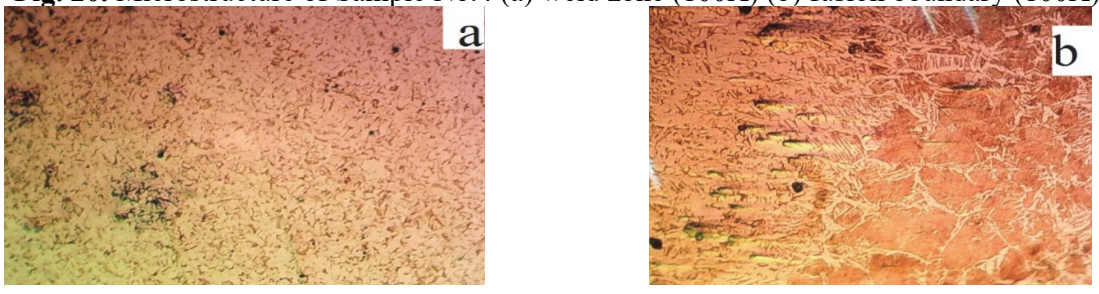

Fig. 21. Microstructure of Sample No.6 (a) weld zone (100X) (b) fusion boundary (100X)

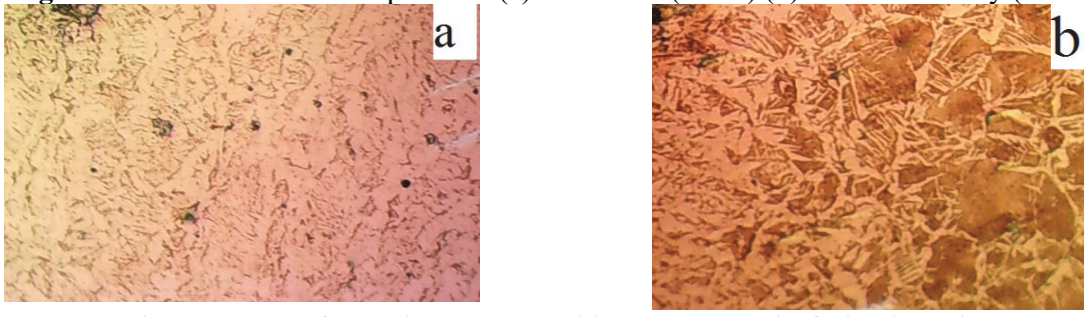

Fig. 22. Microstructure of Sample No.8 (a) weld zone (100X) (b) fusion boundary (100X)

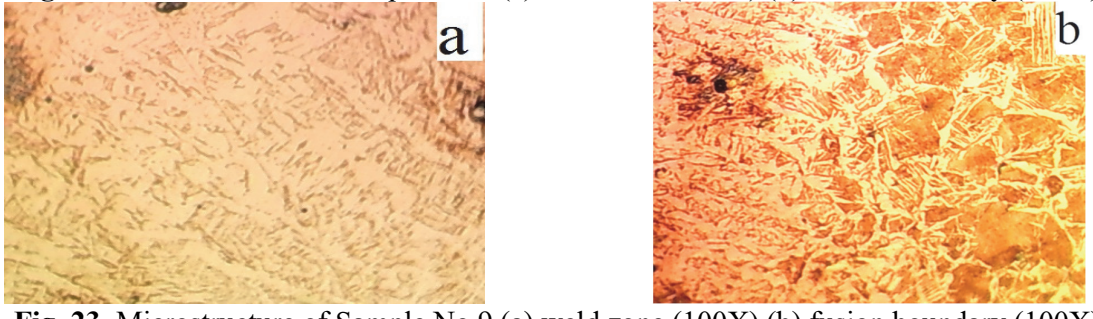

Fig. 23. Microstructure of Sample No.9 (a) weld zone (100X) (b) fusion boundary (100X)

4. Conclusions

The following conclusions may be derived from the experimental investigations:

- As heat input increases in welding operation, absorbed energy of weld metal increases while ultimate tensile strength decreases.
- With increase in energy involved in welding the micro-hardness of weldments decreased in booth transverse & lateral direction.
- At a heat input of 1.872 kJ/mm the micro-hardness is maximum near the weld bead surface in transverse direction and in lateral direction; micro-hardness is maximum at fusion boundary.
- On increasing the heat input value led to grain growth in the weldment zone and results in tempering of martensitic structure.
- From SEM fractograph of fractured surface of tensile test specimen dimples of varying size and shape were observed in the entire fractured surface. It indicates that the fracturing mechanism was ductile.

As the heat input increased it was found from microstructure examination grain size of weldment increases. This leads to increase in ductility and impact strength.

References

Aliha, M. R. M., & Gharehbaghi, H. (2017). The effect of combined mechanical load/welding residual stress on mixed mode fracture parameters of a thin aluminum cracked cylinder. *Engineering Fracture Mechanics*, *180*, 213-228.

Dong, H., Hao, X., & Deng, D. (2014). Effect of welding heat input on microstructure and mechanical properties of HSLA steel joint. *Metallography, Microstructure, and Analysis, 3*(2), 138-146.

Grajcar, A., Różański, M., Stano, S., Kowalski, A., & Grzegorczyk, B. (2014). Effect of heat input on microstructure and hardness distribution of laser welded Si-Al TRIP-type steel. *Advances in Materials Science and Engineering*, 2014.

Li, H., Liu, D., Yan, Y., Guo, N., Liu, Y., & Feng, J. (2018). Effects of heat input on arc stability and weld quality in underwater wet flux-cored arc welding of E40 steel. *Journal of Manufacturing Processes, 31*, 833-843.

Lippold, J. C. (2015). *Welding metallurgy and weldability*. USA: John Wiley & Sons Incorporated.

Miletić, I., Ilić, A., Nikolić, R. R., Ulewicz, R., Ivanović, L., & Sczygiol, N. (2020). Analysis of selected properties of Welded joints of the HSLA steels. *Materials, 13*(6), 1301.

Murti, V. S. R., Srinivas, P. D., Banadeki, G. H. D., & Raju, K. S. (1993). Effect of heat input on the metallurgical properties of HSLA steel in multi-pass MIG welding. *Journal of Materials Processing Technology, 37*(1-4), 723-729.

Muthusamy, C., Karuppiah, L., Paulraj, S., Kandasami, D., & Kandhasamy, R. (2016). Effect of heat input on mechanical and metallurgical properties of gas tungsten arc welded lean super martensitic stainless steel. *Materials Research, 19*(3), 572-579.

Nathan, S. R., Balasubramanian, V., Malarvizhi, S., & Rao, A. G. (2015). Effect of welding processes on mechanical and microstructural characteristics of high strength low alloy naval grade steel joints. *Defence Technology, 11*(3), 308-317.

Njock Bayock, F., Kah, P., Layus, P., & Karkhin, V. (2019). Numerical and experimental investigation of the heat input effect on the mechanical properties and microstructure of dissimilar weld joints of 690-MPa QT and TMCP steel. *Metals, 9*(3), 355.

Prasad, K., & Dwivedi, D. K. (2008). Microstructure and tensile properties of submerged arc welded 1.25 Cr-0.5 Mo steel joints. *Materials and Manufacturing Processes, 23*(5), 463-468.

Sampath, K. (2006). An understanding of HSLA-65 plate steels. *Journal of Materials Engineering and Performance, 15*(1), 32-40.

Shrikrishna, K. A., Sathiya, P., & Goel, S. (2015). The impact of heat input on the strength, toughness, microhardness, microstructure and corrosion aspects of friction welded duplex stainless steel joints. *Journal of Manufacturing Processes, 18*, 92-106.

Soria, A., Álvarez, M., & Carrizalez, M. (2019). Heat input effect in the microstructure on High Strength Low Alloy Steel welded by Laser-GMAW Hybrid Welding, MEMORIAS DEL XXV CONGRESO INTERNACIONAL ANUAL DE LA SOMIM 18 al 20 DE, MAZATLÁN, SINALOA, MÉXICO,1-7.

Taheri-Behrooz, F., Aliha, M. R., Maroofi, M., & Hadizadeh, V. (2018). Residual stresses measurement in the butt joint welded metals using FSW and TIG methods. *Steel and Composite Structures*, *28*(6), 759-766.

Wen, C., Wang, Z., Deng, X., Wang, G., & Misra, R. D. K. (2018). Effect of Heat Input on the Microstructure and Mechanical Properties of Low Alloy Ultra-High Strength Structural Steel Welded Joint. *Steel Research International, 89*(6), 1700500.

Woollin, P. (2007). Postweld heat treatment to avoid intergranular stress corrosion cracking of supermartensitic stainless steels. *Welding in the World, 51*(9), 31-40.

Xue, Q., Benson, D., Meyers, M. A., Nesterenko, V. F., & Olevsky, E. A. (2003). Constitutive response of welded HSLA 100 steel. *Materials Science and Engineering: A, 354*(1-2), 166-179.

Zhu, Z., Han, J., & Li, H. (2015). Effect of alloy design on improving toughness for X70 steel during welding. *Materials & Design, 88*, 1326-1333.